

# Brachistochronic Non-Adiabatic Holonomic Quantum Control

Bao-Jie Liu,<sup>1</sup> Zheng-Yuan Xue,<sup>2,1,\*</sup> and Man-Hong Yung<sup>1,†</sup>

<sup>1</sup>*Institute for Quantum Science and Engineering, and Department of Physics,  
Southern University of Science and Technology, Shenzhen 518055, China*

<sup>2</sup>*Guangdong Provincial Key Laboratory of Quantum Engineering and Quantum Materials,  
GPETR Center for Quantum Precision Measurement, and School of Physics and Telecommunication Engineering,  
South China Normal University, Guangzhou 510006, China*

(Dated: December 21, 2024)

In quantum control, geometrical operations can provide an extra layer of robustness against control errors. However, a limitation of the conventional non-adiabatic holonomic quantum computation (NHQC) is that all of the operations are performed with exactly the same amount of time, even for a small-angle rotation. Furthermore, NHQC requires the driving part of the Hamiltonian to strictly cover a fixed pulse area, making it sensitive to control errors. Here we present an unconventional approach of NHQC, termed B-NHQC, for bypassing these limitations of the conventional NHQC. Specifically, with B-NHQC, almost all non-Abelian geometric gates can be time-optimized by following the brachistochrone curve, minimizing the impact from the environmental decoherence. In addition, the B-NHQC approach avoids the stringent pulse requirement imposed in the conventional NHQC, making it also robust against control errors. Additionally, we demonstrate that B-NHQC is compatible with composed pulses to further enhance the robustness against pulse errors. For benchmarking, we provide a thorough analysis on the performance of B-NHQC under experimental conditions; we found that the gate fidelity can be significantly improved from 98.4% to 99.84% compared with NHQC.

**Introduction.**— Realizing precise and noise-resistant quantum gates are of vital importance to massive quantum computation. Geometric phases depend only on the global properties of the evolution paths, and thus quantum gates based on which are immune to local errors during the evolution [1–3]. Therefore, geometric quantum computation [4–9], where quantum gates are induced by geometric phases of qubits' states, is a promising strategy for fault-tolerant quantum computation. More specifically, a geometric phase can either be a real number, i.e., Abelian, known as the "Berry phase" [10], or a matrix, i.e., non-Abelian holonomy [11], which is the key ingredient in constructing quantum operations for holonomic quantum computation.

For the implementation aspect, dynamical phases will also be induced in general, and thus how to remove or avoid them is an additional problem need to be considered. To this end, holonomic quantum computation based on adiabatic evolution, without the dynamical phase, has been proposed using two dark states in tripod systems [12, 13]. However, the adiabatic condition there implies lengthy gate time, thus the environment-induced decoherence will introduce severe gate infidelity. To overcome this problem, nonadiabatic holonomic quantum computation (NHQC) schemes have been proposed to remove the need of the adiabatic condition [17, 18]. Moreover, the NHQC can be extended to realize arbitrary single-qubit holonomic quantum gate in a single-loop/shot evolution [19–24] and compatible with elementary optimal control techniques [25, 26]. Recently, elementary holonomic quantum gates have been experimentally demonstrated in different platforms, including superconducting circuits [27–30], nuclear magnetic resonance (NMR) [31–33], and nitrogen-vacancy centers in diamond [34–39], etc. However, these NHQC implementations are sensitive to systematic errors due to the stringent requirements on the govern Hamiltonian [40–44].

Here, we present an unconventional approach of NHQC,

called B-NHQC, for breaking the two limitations of the conventional NHQC, which extends the unconventional Abelian geometric scheme [45, 46] to the non-Abelian case. Comparing with previous implementations of conventional NHQC, our scheme is more robust against control induced imperfections, as we remove the fixed pulse area limitation. Moreover, we can combine our model with composite scheme to further enhance the robustness of B-NHQC. Furthermore, our scheme also incorporates with the time-optimal technology [47–50], by solving the quantum brachistochrone equation (QBE), to realize universal holonomic gates with *minimum* time, and thus minimizes the decoherence induced gate infidelity. Finally, we consider a three-level quantum system to explain the working mechanism of B-NHQC. Numerical simulations indicate that our B-NHQC and its' optimization can achieve a significant improvement over the NHQC gates [17, 18] using the experimental parameters.

**General model.**— We consider a general time-dependent Hamiltonian  $H(t)$ . Assume  $\{|\psi_m(t)\rangle\}$  is a complete set of basis, the vectors of which, at each moment of time  $t$ , follow the time-dependent Schrödinger equation (TDSE), i.e.,  $i|\dot{\psi}_k(t)\rangle = H(t)|\psi_k(t)\rangle$ , and thus the time evolution operator  $U(t, 0) = \mathcal{T}e^{-i\int_0^t H(t')dt'} = \sum_m |\psi_m(t)\rangle \langle\psi_m(0)|$ . Meanwhile, we can set a different set of time-dependent basis,  $\{|\phi_k(t)\rangle\}$ , which satisfies the boundary conditions at time  $t = 0$  and  $t = \tau$ ,  $|\phi_k(\tau)\rangle = |\phi_k(0)\rangle = |\psi_k(0)\rangle$ . By aid of  $|\phi_k(t)\rangle$ , we can always write,  $|\psi_m(t)\rangle = \sum_k V_{mk}(t)|\phi_k(t)\rangle$ . Substituting the solutions into TDSE and applying the boundary conditions, we obtain the following unitary transformation matrix at the final time  $t = \tau$  as  $U(\tau) = \sum_{ml} [\mathbf{T}e^{i(\mathbf{A}+\mathbf{K})}]_{ml} |\psi_m(0)\rangle \langle\psi_l(0)|$ , where  $\mathbf{T}$  is time ordering operator, the dynamical and geometric parts are denoted by  $K_{ml} \equiv -\int_0^\tau \langle\phi_m(t)| H(t) |\phi_l(t)\rangle dt$  and  $A_{ml} \equiv \int_0^\tau i \langle\phi_m(t)| \frac{d}{dt} |\phi_l(t)\rangle dt$ . Here, we extend the def-

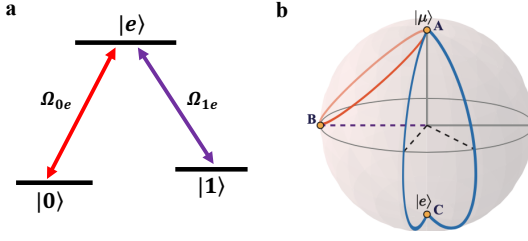


FIG. 1. Illustration of the proposed scheme. (a) The coupling configuration for the single-qubit gates with two microwave fields  $\Omega_{0e}$  and  $\Omega_{1e}$  resonantly coupled to the three levels of a quantum system. (b) Geometric illustration of the proposed B-NHQC gate on the Bloch sphere, where the state  $|\mu\rangle$  undergoes a cyclic evolution  $A \rightarrow B \rightarrow A$ . However, the conventional NHQC takes a cyclic evolution  $A \rightarrow C \rightarrow A$ .

initiation the unconventional geometric phase [45, 46] from the Abelian case to a non-Abelian holonomic case, where the generalized unconventional quantum holonomy satisfies

$$\mathbf{K} = \eta \mathbf{A} + \mathbf{G}, \quad (1)$$

where  $\eta$  is a proportional constant and the matrix  $\mathbf{G}$  depends only on the global geometric feature of the evolution path. Hence, we obtain our target unconventional holonomy in the  $\{|\psi_m\rangle\}$  basis as

$$U(\tau) = \mathbf{T} e^{i[(1+\eta)\mathbf{A} + \mathbf{G}]}. \quad (2)$$

Inevitably, any implementation will suffer from decoherence, which reduces the target gate fidelity, and thus operations with *minimum* time becomes a preferable choice for realizing high-fidelity gates. To realize the fastest geometric gates, we extend the above framework to B-NHQC, by combining it with the time-optimal control technique [47–50], via solving the QBE

$$i\partial F/\partial t = [H, F], \quad (3)$$

where  $F = \partial L_c/\partial H$  and  $L_c = \sum_j \mu_j f_j(H)$ , with  $\mu_j$  being the Lagrange multiplier. Note that, choosing different parameters of the driven Hamiltonian  $H(t)$  makes the evolution of the system follow different paths, but leads to a same unconventional holonomic gate. The path with the minimal time can be obtained by solving the QBE together with TDSE. For a realistic physical systems, there always be a constraint that the energy bandwidth, described by  $f_0(H) = [Tr(H^2) - E^2]/2$ , should be finite.

*Application of B-NHQC.*— We firstly illustrate the implementation of our idea in a three-level system, where the ground state  $|0\rangle$  and  $|1\rangle$  are chosen as logic states of the qubit, while the excited state  $|e\rangle$  as an auxiliary state, as shown in Fig. 1(a). The transitions of  $|0\rangle \leftrightarrow |e\rangle$  and  $|e\rangle \leftrightarrow |1\rangle$  are driven resonantly by two microwave fields, with the amplitudes  $\Omega_{0e}(t)$ ,  $\Omega_{e1}(t)$  and the phases  $\phi_0$  and  $\phi(t)$ , respectively. Assuming  $\hbar = 1$  hereafter, the Hamiltonian of the system is

$$H_1(t) = \frac{\Omega(t)}{2} e^{i\phi(t)} \left( \sin \frac{\theta}{2} e^{i\phi_1} |0\rangle + \cos \frac{\theta}{2} |1\rangle \right) |e\rangle + \text{H.c.}, \quad (4)$$

where  $\phi_1 = \phi_0 - \phi(t)$ ,  $\Omega(t) = \sqrt{\Omega_{0e}^2(t) + \Omega_{1e}^2(t)}$  and  $\tan(\theta/2) = \Omega_{0e}(t)/\Omega_{1e}(t)$ , and the mixing angle  $\theta$  is set to be time-independent for simplicity.

As a set of orthogonal solutions of TDSE  $\{|\psi_m(t)\rangle\}$  can be parameterized with two angles  $\chi(t)$ ,  $\alpha(t)$ , and a global phase  $\zeta(t)$  as

$$\begin{aligned} |\psi_0(t)\rangle &= e^{-i\frac{\zeta(t)}{2}} \left( \sin \frac{\chi}{2} e^{-i\frac{\alpha(t)}{2}} |\mu\rangle + \cos \frac{\chi}{2} e^{i\frac{\alpha(t)}{2}} |e\rangle \right), \\ |\psi_1(t)\rangle &= e^{i\frac{\zeta(t)}{2}} \left( \cos \frac{\chi}{2} e^{-i\frac{\alpha(t)}{2}} |\mu\rangle - \sin \frac{\chi}{2} e^{i\frac{\alpha(t)}{2}} |e\rangle \right), \\ |\psi_2(t)\rangle &= \cos(\theta/2) |0\rangle + \sin(\theta/2) e^{-i\phi_1} |1\rangle, \end{aligned} \quad (5)$$

with  $|\mu_0\rangle = \sin(\theta/2) e^{i\phi_1} |0\rangle + \cos(\theta/2) |1\rangle$ . Taking  $H_1(t)$  in Eq. (4) and  $|\psi_m(t)\rangle$  into TDSE, we obtain

$$\begin{aligned} \dot{\chi}(t) &= \Omega(t) \sin[\phi(t) - \alpha(t)], \\ \dot{\alpha}(t) &= -\cot \chi(t) \Omega(t) \cos[\phi(t) - \alpha(t)], \\ \dot{\zeta}(t) &= \dot{\alpha}(t) \cos \chi(t) - \Omega \cos[\phi(t) - \alpha(t)] \sin \chi(t). \end{aligned} \quad (6)$$

Therefore, the evolution operator is obtained as  $U(t) = \mathcal{T} e^{-i \int_0^t H_1(t') dt'} = \sum_{m=0}^{m=2} |\psi_m(t)\rangle \langle \psi_m(0)|$ .

To construct the geometric phase based holonomic gate, we choose a set of auxiliary states as  $|\phi_1(t)\rangle = e^{if} [\sin \frac{\chi}{2} |\psi_0(t)\rangle + \cos \frac{\chi}{2} |\psi_1(t)\rangle]$  and  $|\phi_2(t)\rangle = |\psi_2\rangle$ , satisfying the boundary conditions  $|\phi_1(0)\rangle = |\phi_1(\tau)\rangle = |\mu\rangle$ . When the cyclic evolution condition  $\zeta(\tau) = 2\pi$  is met with the path  $A \rightarrow B \rightarrow A$  shown in Fig. 1(b), the unconventional holonomic unitary matrix in Eq. (1) on computational subspace  $\{|\phi_1(0)\rangle, |\phi_2(0)\rangle\}$  is

$$U(\tau) = e^{i\mathbf{G}} = \begin{pmatrix} e^{i\gamma} & 0 \\ 0 & 1 \end{pmatrix}, \quad (7)$$

where the control parameters  $\dot{\chi} = 0$  and  $\alpha = \phi$  are chosen. Meanwhile,  $\mathbf{A} = \begin{pmatrix} \gamma - \int_0^T \Omega \sin \chi \cos \chi \sin^2 \zeta dt & 0 \\ 0 & 0 \end{pmatrix}$ ,  $\eta = -1$ , and  $\gamma = \pi - \alpha(\tau)/2$  [51]. Note that Eq. (7) is a holonomy associated with a closed smooth  $C$  in the base space of Grassmann manifold  $G(3, 2)$ , which is the set of two-dimensional computational subspaces within the Hilbert space spanned by the state vectors  $\{|0\rangle, |1\rangle, |e\rangle\}$ .

In the logical qubit subspace  $\{|0\rangle, |1\rangle\}$ ,  $U(\tau)$  leads to a unconventional holonomic single-qubit gate of

$$U(\theta, \phi_1, \gamma) = \exp \left( i \frac{\gamma}{2} \right) \exp \left( -i \frac{\gamma}{2} \mathbf{n} \cdot \boldsymbol{\sigma} \right), \quad (8)$$

which describes a rotation around the  $\mathbf{n} = (\sin \theta \cos \phi, \sin \theta \sin \phi, \cos \theta)$  axis by a  $\gamma$  angle, up to a global phase of  $\gamma/2$ . Since  $\mathbf{n}$  and  $\gamma$  can be arbitrary,  $U(\theta, \phi_1, \gamma)$  can construct arbitrary single-qubit gates, in a single loop evolution. Moreover, our gate scheme can reduce to the conventional NHQC scheme [17, 18], simply by setting  $\chi = \pi/2$  and  $\alpha = 0$ . Then, the evolution satisfies the parallel transport condition, i.e.,  $\gamma_d = 0$ , and the unconventional geometric phase  $\gamma = \pi$  becomes a pure geometric phase.

Recall that for realizing B-NHQC gates, we need to minimize the above gate time by solving the QBE in Eq. (3)

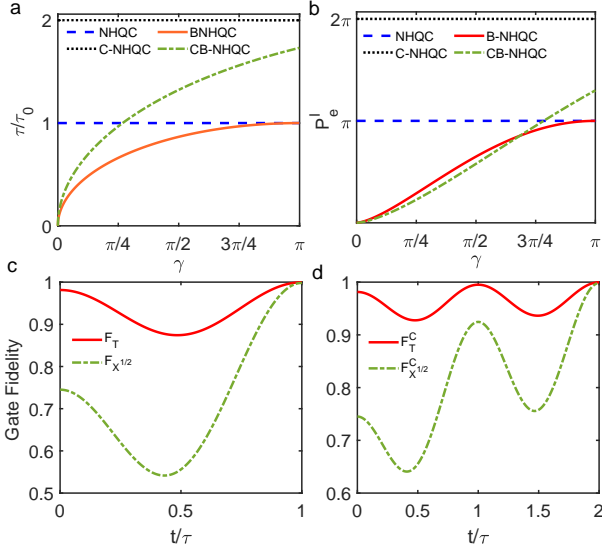


FIG. 2. (a) The dimensionless gate time and (b) the integrated excited-state population  $P_e^I$  of B-NHQC, CB-NHQC, NHQC and C-NHQC schemes with respect to the rotation angle  $\gamma$ . Dynamics of gate fidelities of  $X^{1/2}$  and  $T$  gates in B-NHQC (c) and CB-NHQC (d) schemes.

to reduce the influence of the environmental induced decoherence effect. Here, we can simply set  $\Omega(t) = \Omega_0$  to satisfy the constraint, i.e.,  $f_0(H_1) = [Tr(H_1^2) - \Omega_0^2]/2 = 0$ . Following the Ref. [49–51], by solving the Eq. (3), one minimum-time solution to our purpose is  $\phi(t) = \alpha(t) = 2(\gamma - \pi)t/\pi\tau$ , with the minimum evolution time being  $\tau = 2\sqrt{\pi^2 - (\pi - \gamma)^2}/\Omega_0$ , which decreases with the decrease of the geometric phase  $\gamma$ .

Furthermore, we can enhance the robustness of B-NHQC against systematic control errors by combining it with the composite pulse strategy, which we call CB-NHQC, similar to the case of composite NHQC (C-NHQC) [33, 53]. To achieve this, the CB-NHQC is divided into two parts, i.e.,  $(0, \tau)$  and  $(\tau, 2\tau)$ . During the first interval  $(0 \leq t \leq \tau)$ , we set the phase  $\phi(t) = 2(\gamma/2 - \pi)t/\pi\tau$  corresponding to the evolution operator  $U_1(\theta, \phi_1, \gamma/2)$ . For the second interval,  $\phi'(t) = \pi + 2(\gamma/2 - \pi)t/\pi\tau$  with the evolution operator  $U_2 = -U_1$ . As a result, the obtained CB-NHQC gate is

$$U_C(\theta, \phi_1, \gamma) = -[U_1(\theta, \phi_1, \gamma/2)]^2. \quad (9)$$

Here, we plot the evolution time  $\tau$ , in unit of  $\tau_0 = 2\pi/\Omega_0$ , of B-NHQC, CB-NHQC, NHQC and C-NHQC as a function of their corresponding geometric phases, as shown in Fig. 2(a), which clearly shows that B-NHQC scheme generally has a shortest gate time comparing with other schemes. Moreover, as shown in Fig. 2(b), B-NHQC and CB-NHQC schemes can greatly reduce the integrated excited-state populations  $P_e^I = \int_0^\tau |\langle\psi(t)|e\rangle|^2 dt$  compared with NHQC and C-NHQC corresponding to the initial state  $|\mu\rangle$ , which are beneficial to reduce the excited-state decay.

The performance of our proposal in Eq. (8) can be evalu-

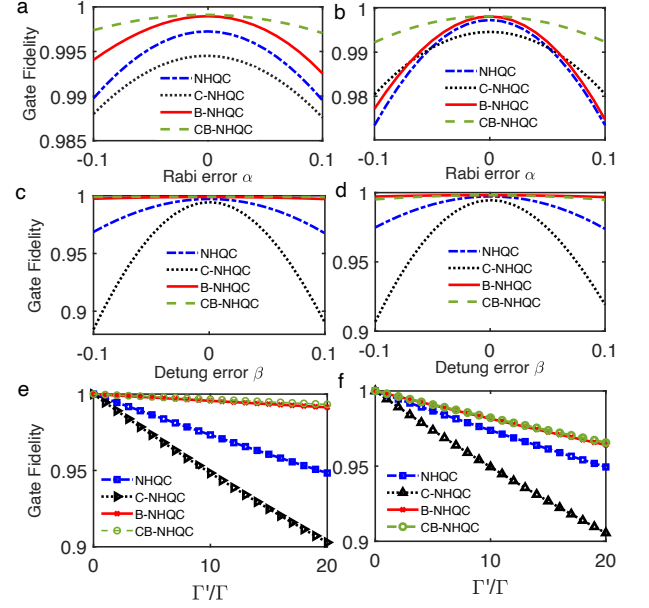


FIG. 3. The gate fidelities under imperfections. The  $T$  and  $X^{1/2}$  gate fidelities for B-NHQC, CB-NHQC, NHQC and C-NHQC cases under the Rabi error (a) and (b), detuning error (c) and (d), decoherence (e) and (f), respectively.

ated by using the quantum master equation of

$$\dot{\rho}_1 = i[\rho_1, H_1] + \frac{\Gamma_-}{2}\mathcal{L}(S_-) + \frac{\Gamma_z}{2}\mathcal{L}(S_z), \quad (10)$$

where  $\rho_1$  is the density matrix of the considered system,  $\mathcal{L}(A) = 2A\rho_1 A^\dagger - A^\dagger A\rho_1 - \rho_1 A^\dagger A$  is the Lindbladian of the operator of  $A$ ,  $S_- = |0\rangle\langle e| + |1\rangle\langle e|$  and  $S_z = |e\rangle\langle e| - |1\rangle\langle 1| - |0\rangle\langle 0|$ ,  $\Gamma_-$  and  $\Gamma_z$  are the decay and dephasing rates of the transmon, respectively. In our simulation, we choose the parameters from the current experiment [52] as  $\Gamma_- = \Gamma_z = \Gamma = \Omega_0/2000$ . We evaluate the  $T$  gate  $U_T = U(0, 0, \pi/4)$  and the  $X^{1/2}$  gate  $U_{X^{1/2}} = U(\pi/2, 0, \pi/2)$ , using the gate fidelity defined by  $F_{T, X^{1/2}} = \frac{1}{2\pi} \int_0^{2\pi} \langle\psi_{T, X^{1/2}}|\rho_1|\psi_{T, X^{1/2}}\rangle d\chi_1$  for a general initial state of  $|\psi(0)\rangle = \cos\chi_1|0\rangle + \sin\chi_1|1\rangle$  with the target state being  $|\psi_{T, X^{1/2}}\rangle = U_{T, X^{1/2}}|\psi\rangle$ . As show in Figs. 2(c) and 2(d), we plot gate fidelities as functions of the time  $\tau$  for 1001 input states with  $\chi_1$  uniformly distributed over  $[0, 2\pi]$ , and the obtained  $T$  gate and  $X^{1/2}$  fidelities in B-NHQC are  $F_{X^{1/2}} = 99.81\%$  and  $F_T = 99.90\%$ , and  $F_{X^{1/2}} = 99.82\%$  and  $F_T = 99.92\%$  in CB-NHQC.

**Robustness.**— We now proceed to show the robustness improvement of our scheme. Firstly, to investigate the robustness against pulse errors, we assume the amplitudes of driven pulse to vary in the range of  $(1 + \alpha)\Omega_0$  with the error fraction  $\alpha \in [-0.1, 0.1]$ . Secondly, we set the frequency detuning error to be  $\Delta|e\rangle\langle e|$  with  $\Delta = \beta\Omega_0$  being static and the fraction is  $\beta \in [-0.1, 0.1]$ . As show Figs. 3, we plot the  $T$  (3a) and  $X^{1/2}$  (3b) gate fidelities of B-NHQC, CB-NHQC, NHQC and C-NHQC as functions of the error fraction  $\alpha$  and  $\beta$  with the relaxation and, find our CB-NHQC strategy is indeed the most robust than the other schemes against both Rabi errors

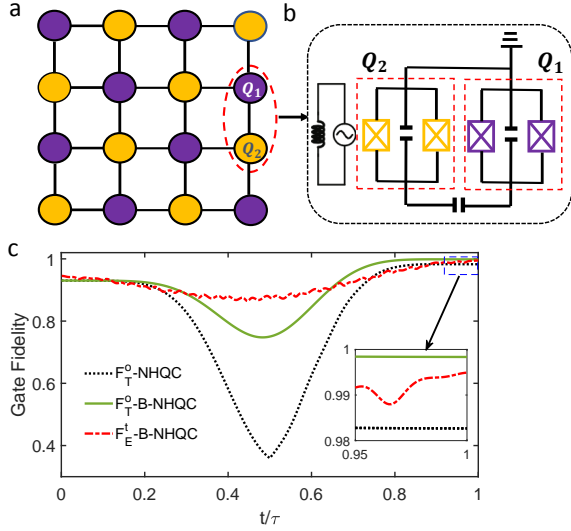


FIG. 4. (a) Scale-up of our physical scheme, the 2D square qubit lattice includes capacitively coupled superconducting transmon qubits, where the transmon qubits are denoted by filled circles. (b) Schematic of our circuit consisting of two capacitively coupled qubits, where  $Q_2$  is biased by an ac magnetic flux to periodically modulate its transition frequency. (c) The  $T$  and two-qubit entangled gate fidelities of B-NHQC as a function of the time.

and detuning errors. Thirdly, we also plot the  $T$  and  $X^{1/2}$  gate fidelities as a function of decoherence rate  $\Gamma$  for above four schemes. As shown in Fig. 3(e) and 3(f), our schemes of B-NHQC and CB-NHQC can greatly suppress the decoherence effect comparing with NHQC and C-NHQC.

*Physical realization on superconducting circuits.*— B-NHQC can be applied to various physical platforms such as superconducting qubits and nitrogen-vacancy centers. Here, we illustrate the implementation of our idea on superconducting circuits, where each transmon serves as a qubit, as shown in Figs. 4(a) and 4(b). We consider the three lowest levels of a transmon qubit, where the ground state  $|g\rangle \equiv |0\rangle$  and the second excited state  $|f\rangle \equiv |1\rangle$  are chosen as our qubit logic states; while the first excited state  $|e\rangle$  as an auxiliary state, the third excited state  $|h\rangle \equiv |2\rangle$  as a leakage state. The corresponding Hamiltonian, in the interaction picture, is approximately given by Eq. (4) [51]. Thus, we can realize B-NHQC single-qubit gate in a single-loop way with a superconducting transmon device.

In our simulation, we choose the simple pulse  $\Omega(t) = \Omega_0 \sin^2(\pi t/\tau)$  to suppress the cross coupling and leakage to higher excited energy levels due to the intrinsic weak anharmonicity  $\kappa$  of the transmon qubit. Using the parameters in current experiments [55, 56],  $\Omega_0 = 2\pi \times 45$  MHz,  $\Gamma = 2\pi \times 4$  kHz, and  $\kappa = -2\pi \times 260$  MHz, we found that the one-qubit  $T$  gate fidelity  $F_T^0$  can be significantly improved from 98.4% to 99.84% compared with NHQC under the same experimental conditions, as shown in Fig. 4(c).

For the universal quantum computation purpose, nontrivial two-qubit gates can be implemented on two capacitively cou-

pled transmons, denoting as  $Q_1$  and  $Q_2$ , as shown in Fig. 4(b). The Hamiltonian can be written as  $H_{\text{sys}} = \sum_{k=1}^2 H_{q_k} + H_{q_c}$  where  $H_{q_k}$  is the single-qubit Hamiltonian and  $H_{q_c}$  is the coupling term. With the lowest four levels of a transmon being considered, the free single-qubit Hamiltonian is  $H_{q_k} = \omega_{q_k} |e\rangle\langle e| + (2\omega_{q_k} + \alpha_k) |1\rangle\langle 1| + (3\omega_{q_k} + 2\alpha_k) |2\rangle\langle 2|$ , where  $\omega_{q_k}$  is the resonant frequency of a transmon,  $\alpha_k$  is the corresponding anharmonicity. Meanwhile, the two-qubit coupling Hamiltonian is  $H_{q_c} = g_{12} (\sigma_1^x \otimes \sigma_2^x + \text{H.c.})$ , where  $g_{12}$  is the static capacitive coupling strength, and  $\sigma_i = (|0\rangle\langle e| + \sqrt{2}|e\rangle\langle 1| + \sqrt{3}|1\rangle\langle 2|)$  is the lower operator for the transmon. To obtain tunable coupling between the two qubits, we add an ac magnetic flux on transmon  $Q_2$  to periodically modulate its eigen-frequency as  $\omega_{q_2}(t) = \omega_{q_2} + \varepsilon \sin(\nu t)$ , where  $\varepsilon$ ,  $\nu$  and  $\varphi$  are the modulation amplitude, frequency, and phase, respectively. Moving into the interaction picture, the interaction Hamiltonian reads [57–60]

$$H_I = g_{12} [\sqrt{2} e^{i(\Delta_1 - \kappa_2)t} e^{i\beta \cos(\nu t + \varphi)} |ee\rangle\langle 01| + \sqrt{2} e^{i(\Delta_1 - \kappa_1)t} e^{i\beta \cos(\nu t + \varphi)} |10\rangle\langle e| + \sqrt{6} e^{i(\Delta_1 - \kappa_2 + 2\kappa_1)t} e^{i\beta \cos(\nu t + \varphi)} |2e\rangle\langle 11| + \sqrt{6} e^{i(\Delta_1 - 2\kappa_2 + \kappa_1)t} e^{i\beta \cos(\nu t + \varphi)} |11\rangle\langle e2| + \text{H.c.}], \quad (11)$$

where  $\Delta_1 = \omega_1 - \omega_2$ ,  $\beta = \varepsilon/\nu$ , and  $|mn\rangle \equiv |m\rangle_1 \otimes |n\rangle_2$ . From the above Hamiltonian, resonant interaction can be induced in both the two or four excitation subspaces, by different choice of the driving frequency  $\nu$ . Ignoring the higher-order oscillating terms, when  $\Delta_1 - \kappa_2 - \mu = \nu$  with a small detuning  $\mu$ , we can get the effective Hamiltonian in the subspace  $\{|01\rangle, |11\rangle, |e2\rangle, |ee\rangle\}$  as,

$$H_e = \frac{1}{2} g'_{12} [e^{-i\mu t} (|ee\rangle\langle 01| + 3e^{i(\kappa_1 - \kappa_2)t} |11\rangle\langle e2|) + \text{H.c.}], \quad (12)$$

where  $g'_{12} = 2\sqrt{2}g_{12}J_1(\beta)$  with  $J_m(\beta)$  being the Bessel function of the first kind.

In the same way as the single-qubit phase gate case, we can realize two-qubit unconventional holonomic entangled gate with minimum time by solving the QBE, and we obtain that  $\mu = 2(\xi - \pi)/\pi$  with a minimum gate time  $\tau_2 = 2\sqrt{\pi^2 - (\pi - \xi)^2}/g'_{12}$ , where  $\xi_1$  and  $\xi_2$  corresponds to the obtained unconventional geometric phase in the subspaces  $\{|01\rangle, |ee\rangle\}$  and  $\{|11\rangle, |e2\rangle\}$ . And the obtained evolution operator  $U_E(\tau_2)$ , i.e., the holonomic entangling gate ( $\xi_1 \neq \xi_2$ ), in the two-qubit basis  $\{|00\rangle, |01\rangle, |10\rangle, |11\rangle\}$  as

$$U_E(\xi_1, \xi_2) = \text{dig}(1, e^{i\xi_1}, 1, e^{i\xi_2}). \quad (13)$$

To evaluate the gate performance, we take the control  $T$  gate  $U_E(\pi/4, -\pi/4)$  as a typical example. Here, we set the parameters [57, 58] of the transmons as  $\kappa_1 = -2\pi \times 220$  MHz,  $\kappa_2 = \kappa$ ,  $\Delta_1 = 2\pi \times 146$  MHz and  $g_{12} = 2\pi \times 10$  MHz. For a general initial state  $|\psi(0)\rangle = (\cos \chi_1 |0\rangle_1 + \sin \chi_1 |1\rangle_1) \otimes (\cos \chi_2 |0\rangle_2 + \sin \chi_2 |1\rangle_2)$ , the two-qubit gate fidelity defined by [60]  $F_E^t = (1/4\pi^2) \int_0^{2\pi} \int_0^{2\pi} \langle \psi_{fs} | \rho_2 | \psi_{fs} \rangle d\chi_1 d\chi_2$  with the target state  $|\psi_E\rangle = U_E |\psi(0)\rangle$ , the gate fidelity of  $U_E$  can be as high as 99.50%, as shown in Fig. 4(c).



*Conclusion.*— We have proposed an unconventional approach of NHQC scheme with non-Abelian geometric phase, which can be compatible with time-optimal control technology to realize the fastest holonomic gate. Comparing with conventional NHQC, our proposal is more robust against the experimental control errors and decoherence. We also presented an explicit way to implement our scheme using a three-level system, and numerically simulated the performance of pulse optimization for superconducting circuits, where the gate fidelity can be significantly improved. Moreover, we discuss how the B-NHQC gate presented here can be applied to two-qubit gates in detail.

We thank T. Chen for helpful discussion. This work is supported by the Key-Area Research and Development Program of Guangdong Province (Grant No.2018B030326001), the National Natural Science Foundation of China (Grant No.11875160 and No.11874156), the Natural Science Foundation of Guangdong Province (Grant No.2017B030308003), the National Key R& D Program of China (Grant No.2016YFA0301803, the Guangdong Innovative and Entrepreneurial Research Team Program (Grant No.2016ZT06D348), the Economy, Trade and Information Commission of Shenzhen Municipality (Grant No.201901161512), the Science, Technology and Innovation Commission of Shenzhen Municipality (Grant No. JCYJ20170412152620376, No. JCYJ20170817105046702, and No. KYTDPT20181011104202253).

---

\* [zyxue83@163.com](mailto:zyxue83@163.com)

† [yung@sustech.edu.cn](mailto:yung@sustech.edu.cn)

- [1] P. Zanardi, and M. Rasetti, Phys. Lett. A **264**, 94 (1999).
- [2] E. Sjöqvist, Physics **1**, 35 (2008).
- [3] Y. Aharonov, and J. Anandan, Phys. Rev. Lett. **58**, 1593 (1987).
- [4] S.-L. Zhu, and P. Zanardi, Phys. Rev. A **72**, 020301(R) (2005).
- [5] J. A. Jones, V. Vedral, A. Ekert, and G. Castagnoli, Nature **403**, 869 (2000).
- [6] S. Berger, M. Pechal, A. A. Abdumalikov, Jr., C. Eichler, L. Steffen, A. Fedorov, A. Wallraff, and S. Filipp, Phys. Rev. A **87**, 060303(R) (2013).
- [7] G. De Chiara and G. M. Palma, Phys. Rev. Lett. **91**, 090404 (2003).
- [8] P. J. Leek, J. M. Fink, A. Blais, R. Bianchetti, M. Goppl, J. M. Gambetta, D. I. Schuster, L. Frunzio, R. J. Schoelkopf, and A. Wallraff, Science **318**, 1889 (2007).
- [9] S. Filipp, J. Klepp, Y. Hasegawa, C. Plonka-Spehr, U. Schmidt, P. Altenkort, and H. Rauch, Phys. Rev. Lett. **102**, 030404 (2009).
- [10] M. V. Berry, Proc. R. Soc. Lond. A **392**, 45 (1984).
- [11] F. Wilczek, and A. Zee, Phys. Rev. Lett. **52**, 2111 (1984).
- [12] L.-M. Duan, J. I. Cirac and P. Zoller, Science **292**, 1695 (2001).
- [13] L.-A. Wu, P. Zanardi, and D. A. Lidar, Phys. Rev. Lett. **95**, 130501 (2005).
- [14] J. Anandan, Phys. Lett. A **133**, 171 (1988).
- [15] Wang X.-B., and M. Keiji, Phys. Rev. Lett. **87**, 097901 (2001).
- [16] S.-L. Zhu, and Z. D. Wang, Phys. Rev. Lett. **89**, 097902 (2002).
- [17] E. Sjöqvist, D. M. Tong, L. M. Andersson, B. Hessmo, M. Johansson, and K. Singh, New J. Phys. **14**, 103035 (2012).
- [18] G. F. Xu, J. Zhang, D. M. Tong, E. Sjöqvist, and L. C. Kwek, Phys. Rev. Lett. **109**, 170501 (2012).
- [19] G. F. Xu, C. L. Liu, P. Z. Zhao, and D. M. Tong, Phys. Rev. A **92**, 052302 (2015).
- [20] E. Sjöqvist, Phys. Lett. A **380**, 65 (2016).
- [21] E. Herterich and E. Sjöqvist, Phys. Rev. A **94**, 052310 (2016).
- [22] P. Z. Zhao, G. F. Xu, Q. M. Ding, E. Sjöqvist, and D. M. Tong, Phys. Rev. A **95**, 062310 (2017).
- [23] G. F. Xu, D. M. Tong and E. Sjöqvist, Phys. Rev. A **98**, 052315 (2018).
- [24] Z.-P. Hong, B.-J. Liu, J.-Q. Cai, X.-D. Zhang, Y. Hu, Z. D. Wang, and Z.-Y. Xue, Phys. Rev. A **97**, 022332 (2018).
- [25] B.-J. Liu, X.-K. Song, Z.-Y. Xue, X. Wang, and M.-H. Yung, Phys. Rev. Lett. **123**, 100501 (2019).
- [26] S. Li, T. Chen, and Z.-Y. Xue, Adv. Quantum Technol., to be published.
- [27] A. A. Abdumalikov, J. M. Fink, K. Juliusson, M. Pechal, S. Berger, A. Wallraff, and S. Filipp, Nature **496**, 482 (2013).
- [28] Y. Xu, W. Cai, Y. Ma, X. Mu, L. Hu, T. Chen, H. Wang, Y. P. Song, Z.-Y. Xue, Z.-Q. Yin, and L. Sun, Phys. Rev. Lett. **121**, 110501 (2018).
- [29] D. J. Egger, M. Ganzhorn, G. Salis, A. Fuhrer, P. Mueller, P. K. Barkoutsos, N. Moll, I. Tavernelli, and S. Filipp, Phys. Rev. Appl. **11**, 014017 (2019).
- [30] T. Yan, B.-J. Liu, K. Xu, C. Song, S. Liu, Z. Zhang, H. Deng, Z. Yan, H. Rong, M.-H. Yung, Y. Chen, and D. Yu, Phys. Rev. Lett. **122**, 080501 (2019).
- [31] G. Feng, G. Xu, and G. Long, Phys. Rev. Lett. **110**, 190501 (2013).
- [32] H. Li, Y. Liu, and G. Long, Sci. China: Phys., Mech. Astron. **60**, 080311 (2017).
- [33] Z. Zhu, T. Chen, X. Yang, J. Bian, Z.-Y. Xue, and X. Peng, Phys. Rev. Appl. **12**, 024024 (2019).
- [34] C. Zu, W.-B. Wang, L. He, W.-G. Zhang, C.-Y. Dai, F. Wang, and L.-M. Duan, Nature (London) **514**, 72 (2014).
- [35] S. Arroyo-Camejo, A. Lazarev, S. W. Hell, and G. Balasubramanian, Nat. Commun. **5**, 4870 (2014).
- [36] Y. Sekiguchi, N. Niikura, R. Kuroiwa, H. Kano, and H. Kosaka, Nat. Photonics **11**, 309 (2017).
- [37] B. B. Zhou, P. C. Jerger, V. O. Shkolnikov, F. J. Heremans, G. Burkard, and D. D. Awschalom, Phys. Rev. Lett. **119**, 140503 (2017).
- [38] N. Ishida, T. Nakamura, T. Tanaka, S. Mishima, H. Kano, R. Kuroiwa, Y. Sekiguchi, and H. Kosaka, Opt. Lett. **43**, 2380 (2018).
- [39] K. Nagata, K. Kuramitani, Y. Sekiguchi, and H. Kosaka, Nat. Commun. **9**, 3227 (2018).
- [40] J. T. Thomas, M. Lababidi, and M. Tian, Phys. Rev. A **84**, 042335 (2011).
- [41] M. Johansson, E. Sjöqvist, L. M. Andersson, M. Ericsson, B. Hessmo, K. Singh, and D. M. Tong, Phys. Rev. A **86**, 062322 (2012).
- [42] S.-B. Zheng, C.-P. Yang, and F. Nori, Phys. Rev. A **93**, 032313 (2016).
- [43] J. Jing, C.-H. Lam, and L.-A. Wu, Phys. Rev. A **95**, 012334 (2017).
- [44] N. Ramberg and E. Sjöqvist, Phys. Rev. Lett. **122**, 140501 (2019).
- [45] S.-L. Zhu and Z. D. Wang, Phys. Rev. Lett. **91**, 187902 (2003).
- [46] J. Du, P. Zou, and Z. D. Wang, Phys. Rev. A **74**, 020302 (2006).
- [47] A. Carlini and T. Koike, Phys. Rev. A **86**, 054302 (2012).
- [48] A. Carlini and T. Koike, J. Phys. A **46**, 045307 (2013).

- [49] X. Wang, M. Allegra, K. Jacobs, S. Lloyd, C. Lupo, and M. Mohseni, *Phys. Rev. Lett.* **114**, 170501 (2015).
- [50] J. Geng, Y. Wu, X. Wang, K. Xu, F. Shi, Y. Xie, X. Rong, and J. Du, *Phys. Rev. Lett.* **117**, 170501 (2016).
- [51] Supplemental Material
- [52] I. Buluta, S. Ashhab, and F. Nori, *Rep. Prog. Phys.* **74**, 104401 (2011).
- [53] G. F. Xu, P. Z. Zhao, T. H. Xing, E. Sjöqvist, and D. M. Tong, *Phys. Rev. A* **95**, 032311 (2017).
- [54] F. Motzoi, J. M. Gambetta, P. Rebentrost, and F. K. Wilhelm, *Phys. Rev. Lett.* **103**, 110501 (2009).
- [55] R. Barends, J. Kelly, A. Megrant, A. Veitia, D. Sank, E. Jeffrey, T. C. White, J. Mutus, A. G. Fowler, B. Campbell, *et al.*, *Nature* (London) **508**, 500 (2014).
- [56] Z. Chen, J. Kelly, C. Quintana, R. Barends, B. Campbell, Y. Chen, B. Chiaro, A. Dunsworth, A. G. Fowler, E. Lucero, *et al.*, *Phys. Rev. Lett.* **116**, 020501 (2016).
- [57] M. Reagor, C. B. Osborn, N. Tezak, A. Staley, G. Prawiroatmodjo, M. Scheer, N. Alidoust, E. A. Sete, N. Didier, M. P. da Silva, *et al.*, *Sci. Adv.* **4**, eaao3603 (2018).
- [58] S. A. Caldwell, N. Didier, C. A. Ryan, E. A. Sete, A. Hudson, P. Karalekas, R. Manenti, M. P. da Silva, R. Sinclair, E. Acala, *et al.*, *Phys. Rev. Appl.* **10**, 034050 (2018).
- [59] X. Li, Y. Ma, J. Han, T. Chen, Y. Xu, W. Cai, H. Wang, Y.P. Song, Z.-Y. Xue, Z.-Q. Yin, and L. Sun, *Phys. Rev. Appl.* **10**, 054009 (2018).
- [60] T. Chen and Z.-Y. Xue, *Phys. Rev. Appl.* **10**, 10, 054051 (2018).